Dual Temperature and pH Responsiveness of Poly(2-(*N*,*N*-dimethylamino)ethyl methacrylate-*co*-*n*-butyl acrylate) Colloidal Dispersions and Their Films

Fang Liu and Marek W. Urban*

Shelby F. Thames Polymer Science Research Center, School of Polymers and High Performance Materials, The University of Southern Mississippi, Hattiesburg, Mississippi 39406

Received March 27, 2008; Revised Manuscript Received June 24, 2008

ABSTRACT: 2-(*N*,*N*-Dimethylamino)ethyl methacrylate (DMAEMA) and *n*-butyl acrylate (nBA) monomers were copolymerized to form p(DMAEMA/nBA) colloidal particles that exhibit pH- and temperature-responsive behavior. Aqueous p(DMAEMA/nBA) colloidal dispersions exhibit second-order lower critical solution temperature (II-LCST) transition, referred to as stimuli-responsive temperature (T_{SR}) for solid films, in the 27−37 °C range manifested by the particle size changes from 148 to 80 nm. Upon pH changes from 2 to 10, the particle size also changed from 205 to 139 nm. When p(DMAEMA/nBA) colloidal particles were allowed to coalesce which was facilitated by the presence of nBA component, the films retained their dual responsiveness and shrink in all the directions at $T > T_{SR}$ while expanding upon pH changes from basic to acidic. Thermodynamic molecular simulations combined with spectroscopic analysis showed that the temperature-responsive behavior results from the collapse of the (dimethylamino)ethyl groups and twisting/buckling of the copolymer backbone, while the pH responsiveness is attributed to protonation/deprotonation of amine functional groups. Molecular simulations also showed that the total volume (V) above T_{SR} decreases by 21.6%, whereas a 13.26% increase occurs at the protonation state, which is in good agreement with the experimental data.

Introduction

Numerous advantages of synthetic polymers capable of responding to external/internal stimuli and their potential of mimicking biological species generated significant scientific and application interests.[1] Among many polymeric systems, probably the most studied synthetic polymer that exhibits temperature responsiveness is poly(*N*-isopropylacrylamide) (PNIPAAm),[2−7] with the low critical solution temperature (LCST) at ∼32 °C. Among the pH-responsive polymers, polyacids, such as poly(acrylic acid)[8] (PAAc), and polybases, like poly(vinylpyridine)[9] (PVP), have been also investigated,[10] and the presence of ionizable pendent groups that may accept or donate protons makes these species pH-responsive. In an effort to achieve simultaneous temperature and pH responses, a common approach is to combine acrylic acid/amine functionalities as pH and acrylamide derivatives as temperature-responsive components[11−13] into one copolymer backbone, thus generating simultaneous pH and temperature responsiveness. Poly(2-(*N*,*N*-dimethylamino)ethyl methacrylate) (PDMAEMA) exhibits such dual responsiveness within itself, where temperature sensitivity results from (dimethylamino)ethyl groups and generates the LCST at around 40 °C,[14,15] and pH responsiveness is attributed to protonation/deprotonation of the tertiary amine side groups.[16,17]

While stimuli-responsive behavior of these and many other polymer systems has been achieved in aqueous solutions where energetic and spatial restrictions can be easily overcome, significant difficulties are present in solids. Either the lack of spatial mobility or high glass transition temperature (T_g) impose limitations on the availability of free volume that is required for network rearrangements to occur. Furthermore, film formation is often inhibited by elevated T_g of many stimuli-responsive homopolymers. In an effort to overcome these limitations, we recently synthesized colloidal particles of poly((*N*-(DL)-(1-hydroxymethyl)propylmethyacrylamide/*n*-butyl acrylate) (p(DL-HMPMA/nBA)) copolymer,[18] which exhibits a broad range of LCST (27−37 °C) and the presence of copolymerized nBA components facilitates coalescence. We refer to these transitions as the second-order low critical solution temperature (II-LCST)[18] in colloidal dispersions, and one of the interesting outcomes of these studies was directional responsiveness of the coalesced p(DL-HMPMA/nBA) films. For solid films, this temperature is referred to as stimuli-responsive temperature (T_{SR}). In view of these findings and considering that the presence of low-T_g components facilitates free volume required for polymer network rearrangements, these studies focus on copolymerization of DMAEMA and nBA monomers to form stable water-dispersible colloidal particles. Part I focuses on the synthesis and stimuli responsiveness of p(DMAEMA/nBA) aqueous colloidal dispersions, whereas part II is devoted to temperature and pH responsiveness of coalesced p(DMAEMA/nBA) films and conformational/dimensional changes resulting from pH and temperature changes.

Experimental Section

2-(*N*,*N*-Dimethylamino)ethyl methacrylate (DMAEMA) was purchased from Polysciences Inc. Hexadecyltrimethylammonium chloride (HTAC) solution was purchased from Fluka Chemical Co. 2,2′-Azobis(isobutyronitrile) (AIBN), *n*-butyl acrylate (nBA), and 0.1 N volumetric standard solutions of sodium hydroxide (NaOH) and hydrochloride acid (HCl) were purchased from Aldrich Chemical Co. 36.7% hydrochloride acid was purchased from VWR Inc.

p(DMAEMA/nBA) copolymer was synthesized using the semicontinuous emulsion polymerization process outlined elsewhere[19] and was adapted for a small scale polymerization. The reaction flask was immersed in a water bath preheated to 75 °C and purged continuously with N_2 gas. The reactor was first charged with 27 mL of double dionized (DDI) water, and after purging N_2 for 30 min, the content was stirred at 300 rpm. At this point, pre-emulsion (DDI, 25 mL; HTAC, 0.155 g; monomers, 5.6 g; and oil-soluble initiator AIBN, 0.065 g) was fed at 0.155 mL/min into the vessel over a period of 3 h. After completion of pre-emulsion feeding, the reaction was continued for additional 3 h. The resulting colloidal

* To whom correspondence should be addressed.

10.1021/ma8006784 CCC: $40.75
Published on Web 08/06/2008

dispersion was filtered after cooling to ambient temperature, and the pH value determined by potentiometric titration was ~8. P(DMAEMA) and p(nBA) homopolymers were prepared using the same method.

Particle size analysis was performed using a Microtrac Nanotrac particle size analyzer (model NPA 250) with an accuracy of ±10 nm. Potentiometric titrations were performed at 22 °C using Orion pH meter model 350 with a glass combination electrode (Orion 9202 BN). Autocalibration against standard buffer solutions was done before titration. Standard HCl and NaOH were utilized to adjust pH values of p(DMAEMA/nBA) aqueous dispersions to be 2, 4, 6, 8, and 10.

Molecular weight was determined using gel permeation chromatography (Waters, Inc.) equipped with a 515 HPLC pump and a 2414 model refractive index detector. Each sample was precipitated in tetrahydrofuran (THF) and eluted through a 5 μm MIXED-C column. Elution times were referenced against polystyrene standards, and molecular weights of the p(DMAEMA/nBA) copolymer and p(DMAEMA) homopolymer were 238 000 and 187 000 g/mol, and the polydispersity index (PDI) values were 1.31 and 1.28, respectively.

Proton NMR (^{1}H NMR) spectra were acquired using the Varian Mercury 300 MHz NMR spectrometer. Typical measurement conditions involved 45° pulse, relaxation delay 1 s, and acquisition time of 1.998 s. The spectrum represents coaddition of 256 scans. For ^{1}H NMR measurement, 4.03% (w/v) of p(DMAEMA/nBA) copolymer was dissolved in dimethyl sulfoxide (DMSO).

Microscopic attenuated total reflectance Fourier transform infrared (ATR FT-IR) spectra were collected on a Bio-Rad FTS-6000 FT-IR single-beam spectrometer set at 4 cm^{-1} resolution equipped with a deuterated triglycine sulfate (DTGS) detector. A 2 mm Ge crystal with a 45° face angle maintaining constant contact pressure between the crystal and the specimens was used. An amount of 1 μL of colloidal dispersion was placed directly on the Ge crystal and allowed to dry at least 1 h to form a layer of film on the crystal. Each spectrum was collected on the film−substrate (F−S) interface with attached heating elements and represented 100 co-added scans ratioed to 100 scans collected on an empty ATR cell. All spectra were corrected for spectral distortions by Q-ATR software using the Urban−Huang algorithm.[20]

Polymeric films were prepared by casting colloidal dispersions onto the poly(tetrafluoroethylene) (PTFE) substrate and allowed to coalescence at 65% relative humidity (RH) for 72 h at 22 °C in an environmental chamber. In a typical experiment, ~200 μm thick films were prepared and 15 × 10 mm sections were used for dimensional change measurements. Each specimen was equilibrated for 4 h at a given temperature before measuring the dimensional changes using a micrometer (Mitutoyo Co.) with a precision of ±0.1 μm. For the vapor exposure experiments, alkaline p(DMAEMA/nBA) films were sealed together with a beaker containing 20 mL of 36.7% HCl in the environment chamber. After 2 h exposure, dimensional changes of resulting films were measured.

Quantum mechanical semiempirical calculations were conducted using Material Studio software (Accelrys Inc., Version 4.1). Computer modeling simulations were performed using a classical (Newtonian) molecular dynamics theory combined with the COMPASS force field conditions. In the first step, we created infinite polymer long chains containing DMAEMA and nBA monomer units using 3D periodic boundary conditions, such that the local thermo-induced flux was set proportional to the local atom density changes and the local thermodynamic driving forces of the chemical potential. In an effort to determine thermodynamic responses of molecular segments, a 23 × 23 × 23 Å periodic unit cell containing 5 polymer chains and 1185 atoms (1185 asymmetric units) was constructed, and temperature was the control parameter to simulate the heat exchange with the environment. This method involves computing NVT (constant number, volume, and temperature) molecular dynamics at a set temperature using 25 000 steps and 25 picoseconds (ps) (dynamic times), followed by another NPT (constant number, pressure, and temperature) molecular dynamics with 50 000 steps and dynamic times 50 ps and then NVE (constant number, volume, and energy) molecular dynamics with 100 000 steps and 100 ps. The purpose of this three-step process is to simulate energy, volume, and conformational changes at different temperatures. The same unit cell was constructed and the same three-step molecular dynamics process was utilized for the simulation of protonation, and the valence state of amine functional groups was the controlled parameter.

Results and Discussion

In an effort to establish chemical makeup resulting from the synthesis of DMAEMA and nBA monomers described in the Experimental Section, IR and ^{1}H NMR analyses were performed. Traces A, B, and C of Figure 1a illustrate ATR FT-IR spectra of p(nBA) and p(DMAEMA) homopolymers and p(DMAEMA/nBA) copolymer, respectively. As seen in trace A, characteristic bands of p(DMAEMA)[21−23] at 2931 (CH_2 asym str) and 2854 cm^{-1} (CH_2 sym str) in the C−H stretching region and the carbonyl ester band at 1730 cm^{-1} (C═O str) as well as the 1566 cm^{-1} (C−N str) bands due to aminoethyl groups are detected. Trace B illustrates the IR spectrum of p(nBA) with the characteristic bands at 2960 (CH_3 asym str), 2873 (CH_3 sym str), and 1734 cm^{-1} (C═O str), whereas trace C illustrates the spectrum of p(DMAEMA/nBA) copolymer. As anticipated, selected bands in the 2900−3000 and 1350−1500 cm^{-1} regions due to C−H stretching and CH_2/CH_3 deformation modes overlap with the p(nBA) and p(DMAEMA) spectra. Characteristic broadening and a shift of the carbonyl ester band at 1732 cm^{-1} with the band due to aminoethyl groups at 1566 cm^{-1} confirms copolymerization. Further evidence of copolymerization is illustrated in the ^{1}H NMR spectrum of p(DMAEMA/nBA) recorded at 25 °C in DMSO. As shown in Figure 1b, typical resonances at 0.85 ($-CH_2-CH_3$) and 3.8−4.2 ppm ($-O-CH_2$) arise from the copolymerization of nBA units,[24] whereas the peaks at 1.2 ($-C-CH_3$), 2.6 ($-CH_2-N$), 2.7 ($-N-(CH_3)_2$)), and 3.8−4.2 ppm ($-O-CH_2$) are due to DMAEMA units.[22,23] The resonance at 2.5 ppm is due to DMSO solvent. These spectroscopic data demonstrate that DMAEMA and nBA monomers are copolymerized for the feed ratio of 1:1 during free radical semicontinuous copolymerization. The reactivity ratios (r_{nBA} = 0.5; r_{DMAEMA} = 1.8)[25] for both monomers suggest that a random DMAEMA-rich p(DMAEMA/nBA) copolymer was prepared, and the copolymerization yield was 75%. The copolymer composition determined from the NMR data was (DMAEMA/nBA) = 0.54/0.46. The remaining parts of this paper will focus on thermal and pH stimuli responsiveness of p(DMAEMA/nBA) colloidal particles in an aqueous (I) and solid states (II).

I. Solution Behavior of p(DMAEMA/nBA) Colloidal Dispersions. Figure 2 illustrates thermal responsiveness of p(DMAEMA/nBA) copolymer and p(DMAEMA) homopolymer colloidal particles as a function of temperature at pH 8. As shown in Figure 2a, curve A, as temperature increases from 22 to 50 °C, the particle size of p(DMAEMA/nBA) particles decreases from 148 to 80 nm which, according to the literature,[10,26,27] was presumably attributed to hydrogen-bonding and hydrophobic interactions. The visual illustration of the particle size changes is illustrated on the enclosed photographs in Figure 2a, where clear and turbidity/translucent dispersions are observed upon reversible cooling and heating cycles of the colloidal solution. However, unlike homopolymer of p(DMAEMA), which exhibits a narrow transition at 40 °C shown as curve B of Figure 2a, the particle size of p(DMAEMA/nBA) copolymer particles decreases gradually over the 27−37 °C temperature range, which is attributed to the presence of nBA units. The first derivative of the particle size curves is plotted in Figure 2b and, as expected, the bell-shaped curve for p(DMAEMA/nBA) is observed, whereas the p(DMAEMA) homopolymer

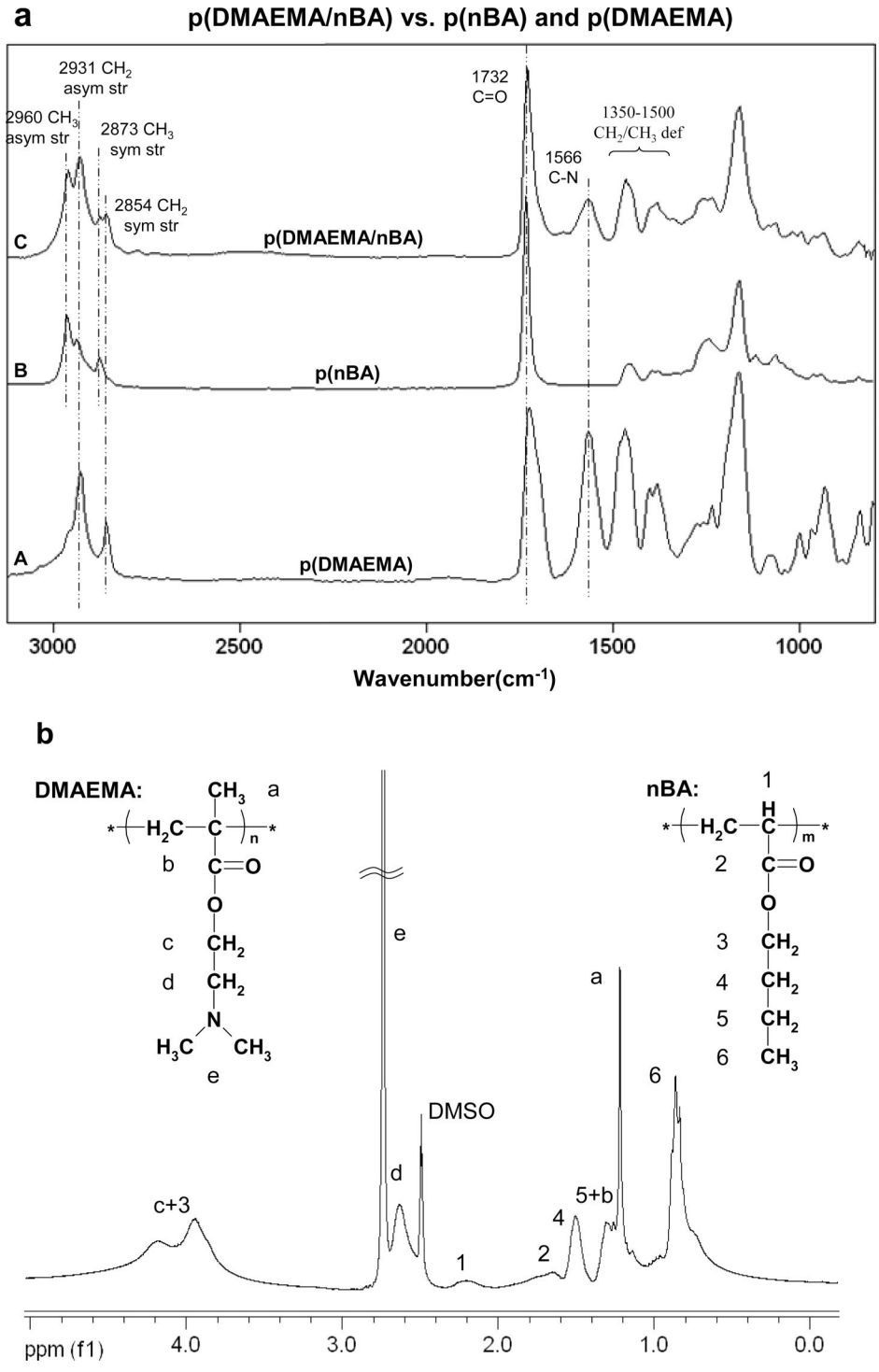

Figure 1. (a) ATR FT-IR spectra of (A) p(DMAEMA), (B) p(nBA), and (C) p(DMAEMA/nBA). (b) ^{1}H NMR spectrum of p(DMAEMA/nBA) in DMSO.

exhibits a single temperature transition. These data illustrate that copolymerization of nBA and DMAEMA monomers broadens and lower the LCST transition maximum. This transition is referred to as the second-order low critical solution temperature (II-LCST) transition.[18]

In an effort to establish pH responsiveness of these dispersions, particle size was analyzed as a function of pH at the 22−50 °C temperature range. Figure 3a illustrates pH and temperature responses of p(DMAEMA/nBA) copolymer colloidal dispersions. As seen, the particle size increases from 139 to 205 nm as the pH values decrease from 10 to 2 at 22 °C. This behavior was attributed to the protonation of the tertiary amine functional groups which causes the p(DMAEMA/nBA) colloidal particles to swell as the copolymer chains repel each other due to electrostatic interactions.[17] Full protonation and swelling are achieved under acidic conditions, which is responsible for significantly larger particle sizes detected at pH values of 2 and 4. Another observation is the shift of the II-LCST transition from 27−37 °C at the pH values of 6−10 to 30−40 °C at pH values of 2−4, as illustrated by plotting the first derivative of the particle size vs temperature in Figure 3b. Although this behavior was attributed to the increased hydrophilicity[7] resulting from ionization of DMAEMA components taking place along the copolymer chains, as further analysis will

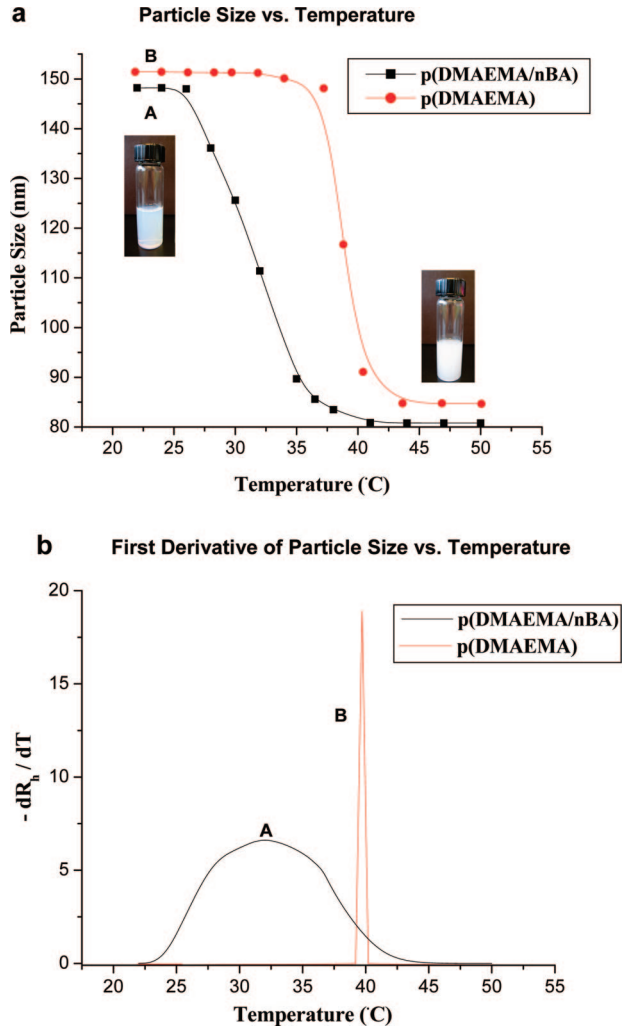

Figure 2. (a) Particle size and (b) its first derivative of (A) p(DMAEMA/nBA) and (B) p(DMAEMA) plotted as a function of temperature.

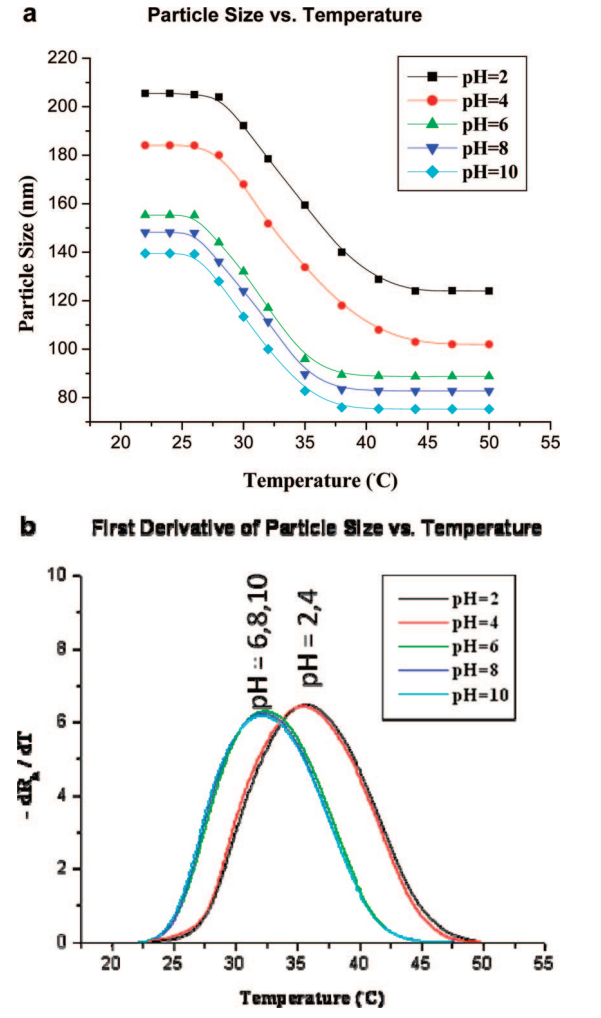

Figure 3. (a) Particle size and (b) its first derivative of p(DMAEMA/nBA) at different pH values plotted as a function of temperature.

show, the side-group mobility plays a significant role in the dimensional changes. To summarize the solution behavior, copolymerization of DMAEMA and nBA monomers maintains thermal and pH responsiveness of colloidal particles, which is the prerequisite for creating dual-responsive solid p(DMAEMA/nBA) films.

II. Solid-State p(DMAEMA/nBA) Behavior. Before we attempt to understand molecular level processes responsible for dual stimuli-responsive behavior, it is a useful exercise to determine 3D dimensional changes in p(DMAEMA/nBA) solid state films as a function of temperature and pH. For that reason, dimensional changes of p(DMAEMA/nBA) films coalesced under different pH aqueous conditions were measured in x (length), y (width), and z (thickness) directions. While Figure 4 illustrates the plots of pH, temperature, and dimensional changes, Table S-1 of the Supporting Information provides the numerical data. As seen, for all pH values, the relative film length, width, thickness (x, y, and z directions), and the total volume diminish as the temperature increases from 22 to 50 °C. Interestingly enough, less pronounced dimensional changes are observed for films with lower pH values, which is attributed to the positively charged tertiary amine groups as they repel each other and resist the shrinkage of p(DMAEMA/nBA) copolymer chains at $T > T_{SR}$. It should be also noted that for the films coalesced from acidic solutions significant dimensional changes are detected at higher temperatures compared to the same films formed from alkaline conditions. For acidic conditions significant shrinkage begins at 30 °C, whereas for alkaline at 28 °C. These changes correspond to the shift of the T_{SR} due to pH changes and agree with the data discussed in Figure 3.

To determine the 3D directional response of p(DMAEMA/nBA) films to environmental pH changes coalesced films were exposed to HCl vapors. The reactions leading to protonation and the resulting dimensional changes are depicted in Figure 5. As illustrated, after HCl exposure (Experimental Section provides details of the experimental conditions), alkaline p(DMAEMA/nBA) films show expansions in x (length), y (width), and z (thickness) directions, which results in the total of an 18% volume increase. At the same time, the relative film length, width, and thickness increase by 3.3%, 3.2%, and 11.2%, respectively. These dimensional changes are summarized in Table 1, and the overall dimensional expansion is attributed to the protonation of tertiary amine side groups which force the polymer backbone to expand and minimize repulsion around the positive charged centers.

While the above discussion centered around dual responsiveness leading to macroscopic changes of p(DMAEMA/nBA) films, the main question is what molecular entities are responsible for these observations. Figure 6 illustrates ATR FT-IR spectra of p(DMAEMA/nBA) copolymer films as a function of pH changes. As seen, the bands at 2706 (N−H str), 2516, 2480 ($N-H^+$ str), and 1100−930 cm^{-1} ($N-H^+$ def) due to the quaternary amine salts are detected under acidic conditions, which confirm the protonation reactions generating positive charged quaternary amine functional groups. Interestingly enough, the bands at 2931 (CH_2 asym str), 2854 (CH_2 sym str),

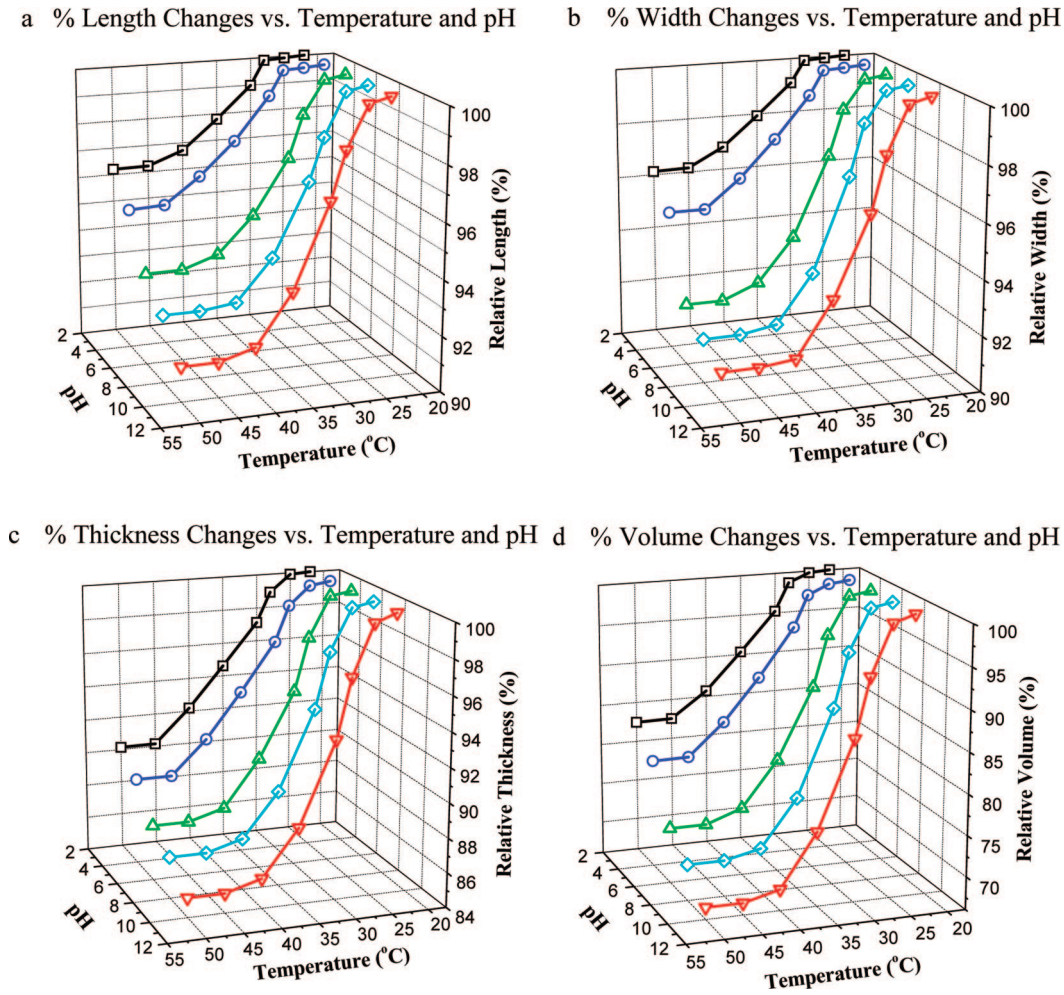

Figure 4. 3D directional thermal and pH response of p(DMAMEA/nBA) films: (a) film length, (b) film width, (c) film thickness, and (d) total film volume changes plotted as a function of temperature and pH: (□) pH = 2; (○) pH = 4; (Δ) pH = 6; (◇) pH = 8; (▽) pH = 10.

Table 1. Dimensional Changes of p(DMAEMA/nBA) Films Exposed to HCl Vapor

	rel length (%)	rel width (%)	rel thickness (%)	rel vol (%)
basic	100	100	100	100
acidic	103.3	103.2	111.2	118.6

and 1566 cm^{-1} (C−N str) due to (dimethylamino)ethyl functional groups of DMAEMA units decrease as the pH changes from 10 to 2. This is attributed to changes of amine groups from nonprotonated to fully protonated state, driven by inversion between hindered amines isomers, as the lone pair of electrons of the tertiary amine have been replaced by the hydrogen atoms in quaternary ammonium ions.

Because pH changes significantly affect the copolymer chains structure and hybridization state, the next question is how these changes will influence p(DMAEMA/nBA) thermal responsiveness. Again, ATR FT-IR spectra of p(DMAEMA/nBA) copolymer films at various pH values were measured as a function of temperature, and the results are summarized in Figure 7. As seen, for p(DMAEMA/nBA) films at pH values of 2 and 4, the bands at 2706 (N−H str), 2516, 2480 ($N-H^+$ str), 1566 (C−N str), and 1100−930 cm^{-1} ($N-H^+$ def) decrease. However, for alkaline p(DMAEMA/nBA) films (Figure 6d,e), the bands at 2931 (CH_2 asym str), 2854 (CH_2 sym str), and 1566 cm^{-1} (C−N str) decrease significantly faster with temperature. At pH = 6, p(DMAEMA/nBA) films are in the partially protonated state; thus, the band intensities decrease for both acidic and alkaline conditions. As anticipated, these changes are attributed to the rearrangements and collapse of polymeric chains above T_{SR}. It should be also noted that, regardless of whether protonated (acid) or nonprotonated (basic), the band intensities decrease is mainly attributed to the (dimethylamino)ethyl functional groups of the DMAEMA component. Moreover, no intensity decreases are observed for the C−H stretching vibrations at 2960 (CH_3 asym str) and 2873 cm^{-1} (CH_3 sym str) of nBA units, thus indicating that the conformational changes above T_{SR} occur within the DMAEMA moiety of the copolymer, while nBA segments, specifically the butyl ester pendant groups, participate in the conformational changes.

To further understand molecular changes and dynamics of p(DMAEMA/nBA) films to pH and temperature responses, computer modeling experiments using molecular thermodynamics simulations were employed. Infinite polymer long chains were created by packing energy-minimized DMAEMA/nBA units in a random sequence under 3D periodic boundary conditions, and details of the computational analysis are provided in the Experimental Section. Visualizations of the simulation results are depicted in Figure 8. As temperature increases above T_{SR}, the unit cells become denser and significant conformational changes occur. As a result of the chain collapse in response to temperature changes, the calculated total energy (G) of the system depicted in Figure 8, which comprises of the potential (E_{pot}) and kinetic energy (E_{kin}), increases by 223 kcal/mol (from 2753 to 2976 kcal/mol). At the same time, E_{pot} changes by 131 kcal/mol (from 1668 to 1799 kcal/mol) and E_{kin} by 92 kcal/mol (from 1084 to 1176 kcal/mol). Since the E_{pot} accounts for conformational changes of the unit cell and E_{kin} for the kinetic energy which is proportional to temperature,

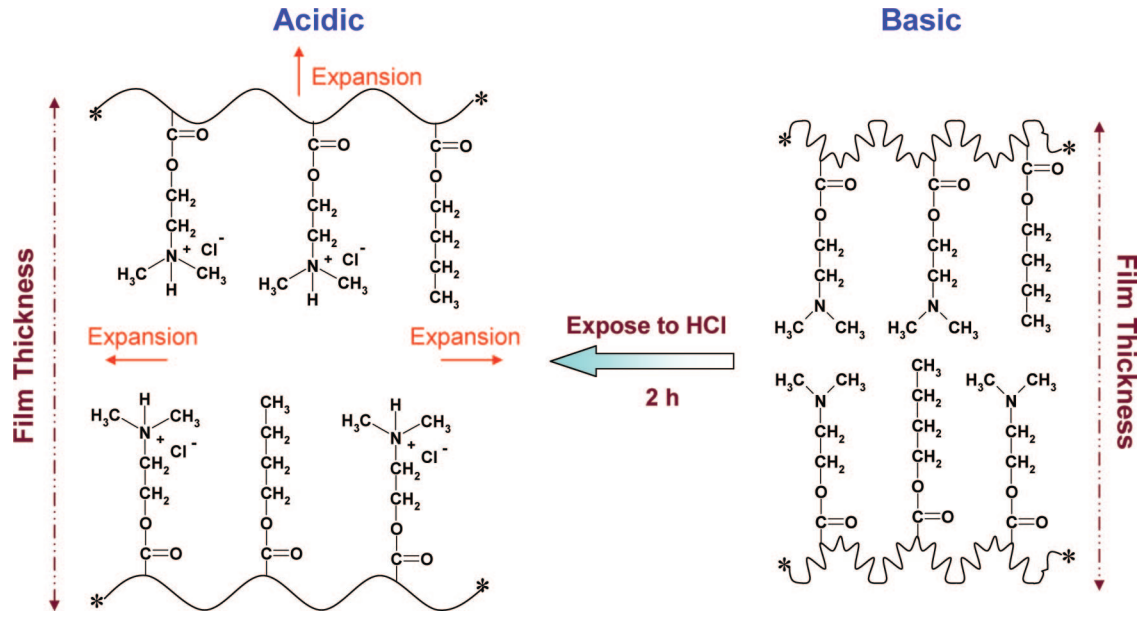

Figure 5. 3D directional response of p(DMAEMA/nBA) films expose to HCl vapor upon protonation reactions.

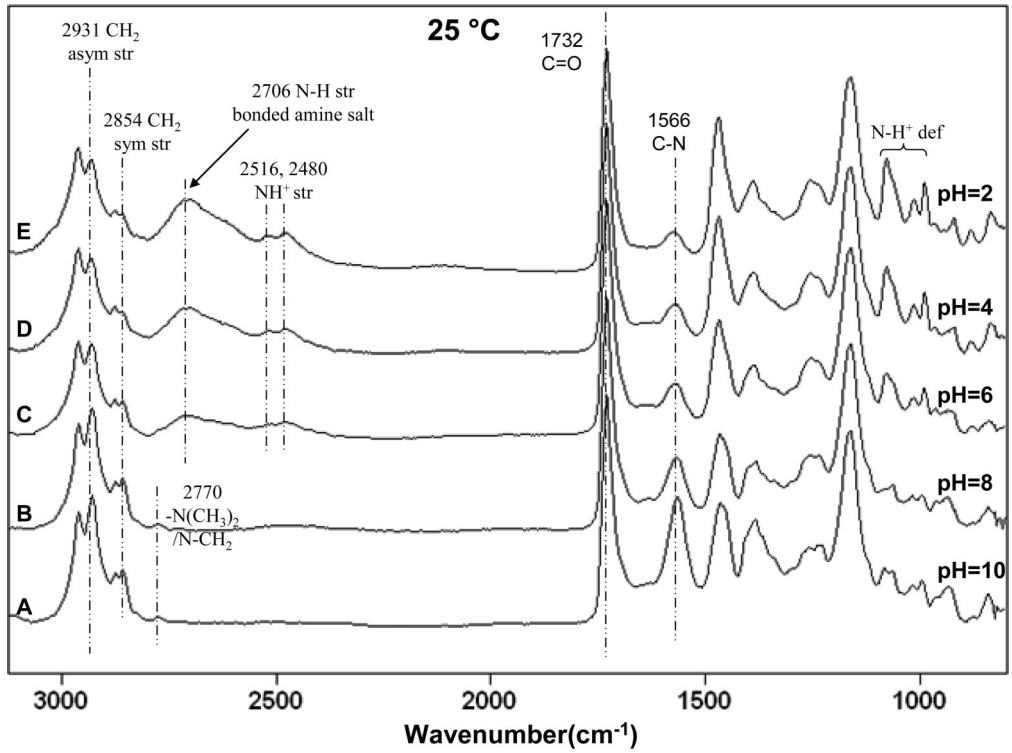

Figure 6. ATR FT-IR spectra of p(DMAEMA/nBA) recorded as a function of pH at 25 °C: A, pH = 10; B, pH = 8; C, pH = 6; D, pH = 4; E, pH = 2.

the larger E_{pot} changes suggest that the collapse of the copolymer chains at $T > T_{SR}$ results in significant conformational changes. Furthermore, molecular dynamic simulations show that during this process, the volume (V) decreases by 21.6% (from 12.15 to 9.52 nm^3), which is in agreement with the experimental data (29.6%) discussed in Figure 4. However, in the case of protonation, the unit cells become less crowded and the copolymer chains extend outside the unit cell. In this case, the calculated energies do not show significant changes, but the volume increases by 13.2% (from 12.15 to 13.75 nm^3), which also agrees with the experimental data (18.6%). The insets A, A′, and A″ of Figure 8 depict predicted conformational changes along the polymer backbone axis (dashed line). As seen in inset A′, at $T = 45$ °C (above T_{SR}) butyl ester side groups still occupy a significant volume, while (dimethylamino)ethyl functional groups of DMAEMA units collapse to form bulky spheres. It is also apparent that the copolymer backbone twists and buckles inward which is another contributing factor to the overall volume decrease. In the protonated state shown as inset A″ of Figure 8, the side groups are repelled away from each other and stretch out in all x, y, and z directions. Also, amine groups before and after protonation are depicted in insets B and B′. It should be noted that numerous studies of polymeric solutions with thermal sensitivity indicated that H bonding is the primarily source for stimuli responsiveness. Both experimental and theoretical data shown in this study clearly indicate that it is not necessary to have hydrogen donor/acceptor groups for thermal and pH responsiveness in polymeric films. In the case of p(DMAEMA/

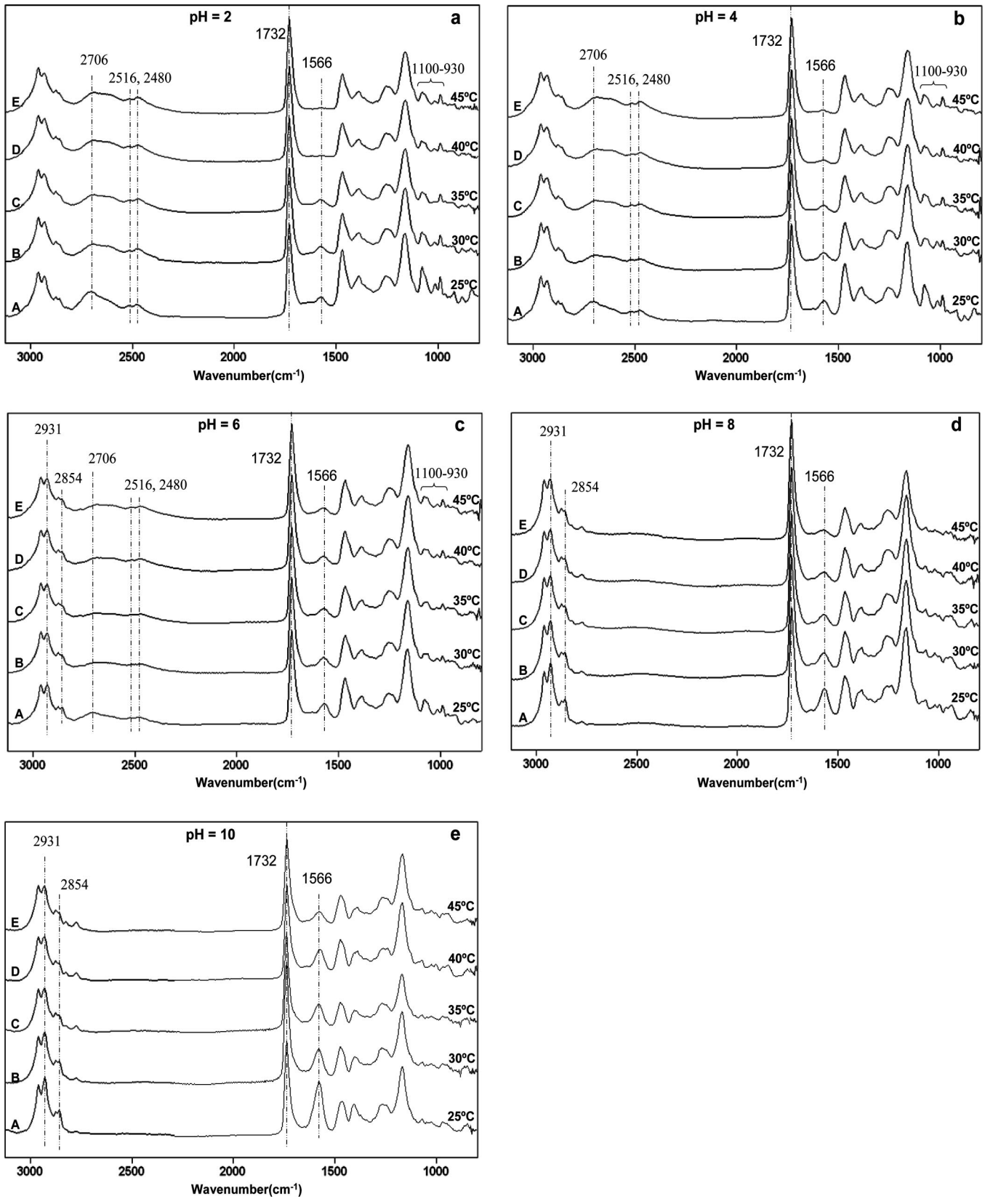

Figure 7. ATR FT-IR spectra of p(DMAEMA/nBA) films at different pH values: (a) pH = 2, (b) pH = 4, (c) pH = 6, (d) pH = 8, and (e) pH = 10, recorded as a function of temperature. Trace A, 25 °C; B, 30 °C; C, 35 °C; D, 40 °C; E, 45 °C.

n-BA) the collapse of the DMAEMA units and buckling of the polymer backbone results from the minimum potential energy changes that causes conformational changes. Furthermore, numerous studies on temperature-sensitive PNIPAAm thin films showed single-directional responsiveness.[5−7] In contrast, for thick p(DMAEMA/n-BA) films developed in this study there is three directional responsiveness sensitive to temperature and pH changes.

It should be pointed out that in the previous studies[18] on p(DL-HMPMA/nBA) films the shrinkage occurred in $x-y$ directions, while expansion in the z direction at $T > T_{SR}$ was observed. This behavior was attributed to the buckling of the

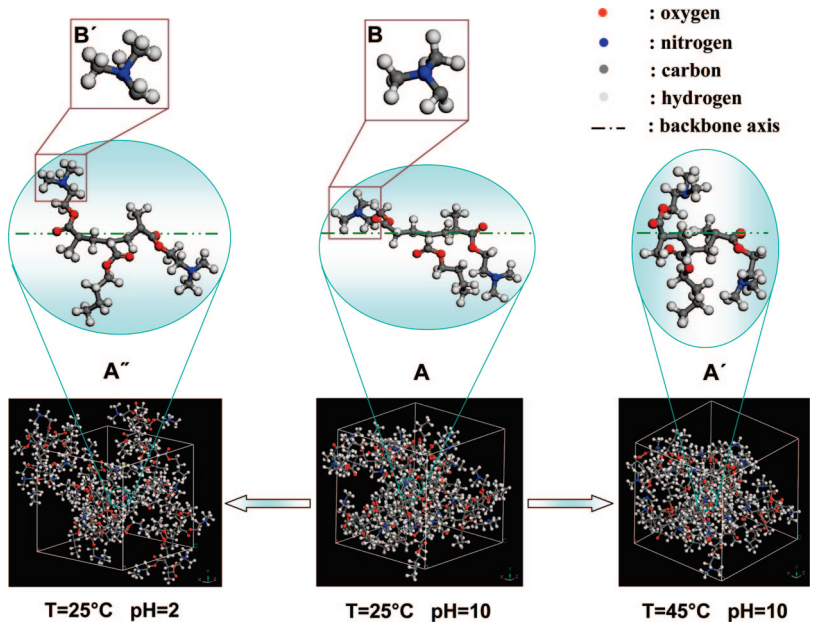

Figure 8. Results of computer simulations representing volume and conformational changes resulting from temperature and valence changes. Insets A, A′, and A″ illustrate molecular conformation below and above T_{SR} as well as upon protonation. Insets B and B′ illustrate the hybridization states of amine groups before and after protonation.

copolymer backbone and orientational changes of the side groups from preferrentially parallel to perpendicular orientations. However, for p(DMAEMA/nBA) films, the shrinkage in all directions and no significant orientational changes of side groups are observed. These differences result from the presence of amide side groups in DL-HMPMA and ester side groups in DMAEMA. The latter exhibits the least possibility of forming inter/intramolecular interactions with itself or butyl ester pendant groups of nBA units. Thus, conformational changes in the T_{SR} transition range may have a lesser effect on the overall orientational changes of the side groups. It should be also noted that, except for ester, amine functionalities are present along one side of the group in DMAEMA to provide pH responsiveness. As a result, the side-group orientation will be random when (dimethylamino)ethyl ester groups respond to the temperature changes. In the same manner, when amine groups respond to pH changes, the ester groups will randomize the orientation of the side groups. As a consequence, no specific side groups orientational changes are detected in p(DMAEMA/nBA) films upon pH or temperature changes.

Conclusions

In these studies novel p(DMAEMA/nBA) colloidal particles as well as coalesced films that retain temperature and pH responsiveness were prepared. The particle size of p(DMAEMA/nBA) aqueous dispersions diminishes from 148 to 80 nm as the temperature increases, but when pH decreases from 10 to 2, the particle size increases from 139 to 205 nm. Coalesced films obtained from colloidal particles of p(DMAEMA/nBA) also show pH- and temperature-responsive behaviors. Spectroscopic data show that the pH-responsive behavior is attributed to the hybridization state changes of amine groups as a result of protonation/deprotonation reactions, whereas the temperature response is attributed to the collapse of (dimethylamino)ethyl functional groups in DMAEMA. Computer modeling experiments showed that total volume (V) increases by 13.2% and decreases by 21.6% at the protonation and $T > T_{SR}$ states, respectively, which are in agreement with the 3D dimensional experimental data: expansion upon pH changes and shrinkage in all the directions upon temperature changes occur.

Acknowledgment. This work was primarily supported by the MRSEC Program of the National Science Foundation under Award DMR 0213883 and partially by the DMR 0215873 Major Research Instrumental (MRI) Program.

Supporting Information Available: Values of the relative % length, width, thickness, and volume changes measured as a function of temperature and pH for p(DMAEMA/nBA) films. This material is available free of charge via the Internet at http://pubs.acs.org.

References and Notes

(1) Urban, M. W. *Stimuli-Responsive Polymeric Films and Coatings*; American Chemical Society: Washington, DC, 2005.
(2) Pelton, R. H. *Colloids Surf., B* **1986**, *20*, 247–256.
(3) Pelton, R. H. *Adv. Colloid Interface Sci.* **2000**, *85*, 1–33.
(4) Alarcon, C.; Pennadam, S.; Alexander, C. *Chem. Soc. Rev.* **2005**, *34*, 276–285.
(5) Wang, W.; Troll, K.; Kaune, G.; Metwalli, E.; Ruderer, M.; Skrabania, K.; Laschewsky, A.; Roth, S. V.; Papadakis, C. M.; Muller-Buschbaum, P. *Macromolecules* **2008**, *41*, 3209.
(6) Hirata, I.; Okazaki, M.; Iwata, H. *Polymer* **2004**, *45*, 5569.
(7) Nykanen, A.; Nuopponen, M.; Laukkanen, A.; Hirvonen, S.-P.; Rytela, M.; Turunen, O.; Tenhu, H.; Mezzenga, R.; Ikkala, O.; Ruokolainene, J. *Macromolecules* **2007**, *40*, 5827.
(8) Philippova, O.; Hourdet, D.; Audebert, R.; Khokhlov, A. *Macromolecules* **1997**, *30*, 8278.
(9) Gohy, J.; Lohmeijer, B.; Varshney, S.; Decamps, B.; Leroy, E.; Boileau, S.; Schubert, U. *Macromolecules* **2002**, *35*, 9748.
(10) Luzinov, I.; Minko, S.; Tsukruk, V. V. *Prog. Polym. Sci.* **2004**, *29*, 635–698.
(11) Pinkrah, V.; Snowden, M.; Mitchell, J.; Seidel, J.; Chowdhry, B.; Fern, G. *Langmuir* **2003**, *19*, 585.
(12) Chen, G.; Hoffman, A. *Nature (London)* **1995**, *373*, 49.
(13) Hoffman, A.; Stayton, P.; Bulmus, V.; Chen, G.; Chen, J.; Cheung, C.; Chilkoti, A.; Ding, Z.; Dong, L.; Fong, R.; Lackey, C.; Long, C.; Miura, M.; Morris, J.; Murthy, N.; Nabeshima, Y.; Park, T.; Press, O.; Shimoboji, T.; Shoemaker, S.; Yang, H.; Monji, N.; Nowinski, R.; Cole, C.; Priest, J.; Harris, J.; Nakamae, K.; Nishino, T.; Miyata, T. *J. Biomed. Mater. Res., Part A* **2000**, *52*, 577.
(14) Okubo, M.; Ahmad, H.; Suzuki, T. *Colloid Polym. Sci.* **1998**, *276*, 470.
(15) Burillo, G.; Bucio, E.; Arenas, E.; Lopez, G. *Macromol. Mater. Eng.* **2007**, *292*, 214.

(16) Lee, A.; Butun, V.; Vamvakaki, M.; Armes, S. P.; Pople, J.; Gast, A. *Macromolecules* **2002**, *35*, 8540.
(17) Plunkett, K. N.; Moore, J. S. *Langmuir* **2004**, *20*, 6535.
(18) Liu, F.; Urban, M. W. *Macromolecules* **2008**, *41*, 352.
(19) Lestage, D.; Urban, M. W. *Langmuir* **2005**, *21*, 2150–2157.
(20) Urban, M. W. *Attenuated Total Reflectance Spectroscopy of Polymers. Theory and Practice*; American Chemical Society: Washington, DC, 1989.
(21) Kim, D. J.; Lee, K.; Chi, Y. S.; Kim, W.; Paik, H.; Choi, I. S. *Langmuir* **2004**, *20*, 7904.
(22) Liu, Q.; Yu, Z.; Ni, P. *Colloid Polym. Sci.* **2004**, *282*, 387.
(23) Heijl, J.; Du Prez, F. *Polymer* **2004**, *45*, 6771.
(24) Pang, X. A.; Sun, H. M.; Shen, Q. *Polymer* **2004**, *45*, 4029.
(25) Brandrup, J.; Immergut, E. H. *Polymer Handbook*; John Wiley & Sons: New York, 1975.
(26) Gil, E. S.; Hudson, S. M. *Prog. Polym. Sci.* **2004**, *29*, 1173–1222.
(27) Aoyagi, T.; Ebara, M.; Sakai, K.; Okano, T. *Macromolecules* **2000**, *33*, 8312–8316.

MA8006784